

Final Draft
of the original manuscript:

Balk, M.; Behl, M.; Lendlein, A.:
**Actuators Based on Oligo[(epsilon-caprolactone)-co-glycolide] with
Accelerated Hydrolytic Degradation.**
In: MRS Advances. Vol. 5 (2020) 12 - 13, 655 - 666.
First published online by Cambridge University Press: 02.12.2019

DOI: 10.1557/adv.2019.447
<https://dx.doi.org/10.1557/adv.2019.447>

Actuators Based on Oligo[(ϵ -caprolactone)-*co*-glycolide] with Accelerated Hydrolytic Degradation

Maria Balk¹, Marc Behl¹, Andreas Lendlein^{1,2*}

¹ Institute of Biomaterial Science, Helmholtz-Zentrum Geesthacht, Teltow, Germany

² Institute of Chemistry, University of Potsdam, Potsdam, Germany

*Correspondence to: Prof. Andreas Lendlein

Institute of Biomaterial Science, Helmholtz-Zentrum Geesthacht, Kantstr. 55, 14513 Teltow, Germany

Email: andreas.lendlein@hzg.de

Phone: +49 (0)3328 352-235

ABSTRACT

Polyester-based shape-memory polymer actuators are multifunctional materials providing reversible macroscopic shape shifts as well as hydrolytic degradability. Here, the function-function interdependencies (between shape shifts and degradation behaviour) will determine actuation performance and its life time.

In this work, glycolide units were incorporated in poly(ϵ -caprolactone) based actuator materials in order to achieve an accelerated hydrolytic degradation and to explore the function-function relationship. Three different oligo[(ϵ -caprolactone)-*co*-glycolide] copolymers (OCGs) with similar molecular weights ($10.5 \pm 0.5 \text{ kg}\cdot\text{mol}^{-1}$) including a glycolide content of 8, 16, and 26 mol% (ratio 1:1:1 wt%) terminated with methacrylated moieties were crosslinked. The obtained actuators provided a broad melting transition in the range from 27 to 44 °C. The hydrolytic degradation of programmed OCG actuators (200% of elongation) resulted in a reduction of sample mass to 51 wt% within 21 days at pH = 7.4 and 40 °C. Degradation results in a decrease of T_m associated to the actuating units and increasing T_m associated to the skeleton forming units. The actuation capability decreased almost linear as function of time. After 11 days of hydrolytic degradation the shape-memory functionality was lost. Accordingly, a fast degradation behaviour as required, e.g., for actuator materials intended as implant material can be realized.

INTRODUCTION

Shape-memory polymer actuators are polymeric systems capable of directed reversible movements, which are controlled by an external input signal like changes in temperature. These systems are reprogrammable and can be utilized for a broad range of applications, e.g. as smart breathable textiles, microvalves for microfluidic systems, or as artificial muscles for biomimetic robots [1-6]. The reversible shape shifts of these actuators can be realized in semi-crystalline copolymer networks, in which actuation domains (semi-crystalline domains with a low melting temperature T_m) enable a melting-induced contraction and crystallization-induced elongation [7-9]. The skeleton domains (crystalline domains with a higher T_m) include the geometric information about the intended reversible macroscopic movement according to the resulting polymer chain orientation during a thermomechanical treatment (programming procedure). Once, the temperature is changed between T_{low} (below T_m of actuator domain) and T_{sep} (separation temperature, between T_m s of actuator and skeleton domains) a macroscopic and reversible shape shift between shape A (at T_{sep}) and shape B (at T_{low}) can be obtained for multiple times. Here, the performance of the movements is controlled by the changes in temperature, its kinetics, as well as the degradation behaviour of the actuator material. Once, degradation of an actuator system occurs, the function-function relationship (between reversible shape shifts and degradation) will determine the performance of macroscopic motions. In a degradation experiment (accelerated degradation conditions, pH = 13, $T = 40$ °C) on oligo(ϵ -caprolactone) based actuators, the performance of directed movements decreased as function of degradation time resulting in the loss of functionality within 105 days, at which 25 wt% of the actuator material was degraded [10]. As for some specific applications of such multifunctional material systems a significant lower lifetime can be required, the degradation rate especially under physiological conditions has to be increased, whereby the actuation performance will be controlled by the function-function interdependency.

In this work we explored, whether an actuator material with accelerated hydrolytic degradability can be created, in which the performance of actuation is controlled by the degradation of the actuator unit. A polymer network based on copolymers of ϵ -caprolactone (providing the creation of semi-crystalline domains) and diglycolide (enabling a fast hydrolytic degradation [11]) including different contents of glycolide was selected. As the introduction of glycolide units reduces the crystallinity and melting transition of the polymer chains, copolymers with a high content of glycolide will preferentially act as actuation domains, whereby copolymers generating the skeleton domain contain a lower content of these fast degrading ester units. Degradation experiments were performed utilizing programmed samples (200% of elongation) at pH = 7.4 (using a phosphate buffer saline solution - PBS) to investigate the actuator lifetime. As temperature for degradation, $T_{sep} = 40$ °C was selected. T_{sep} is located within the broad melting range of the oligo[(ϵ -caprolactone)-*co*-glycolide] (OCG) polymer networks and divides the actuation and skeleton forming domains resulting in shape A of the actuator system during programming and at the same time is close to physiological conditions. In the following, we discuss the influence of hydrolytic degradation on sample mass, swelling behaviour, thermal properties, as well as the interdependencies between the degradation behaviour and the shape-memory actuation capability as function of time.

EXPERIMENTAL

Materials

Oligo[ϵ -caprolactone-*co*-glycolide] diols (OCG-diOH) were synthesized by ring-opening polymerization of ϵ -caprolactone and diglycolide according to the procedure explained in reference [12]. In brief, the dried ϵ -caprolactone and diglycolide were placed in a Schlenk flask and polymerized at 130 °C under inert conditions using butanediol as initiator and dibutyl tin oxide as catalyst. After 24 h the cooligomers were precipitated from hexane and dried until constant weight was achieved. The OCG-diOHs were modified with 2-isocyanatoethyl methacrylate (IEMA, Sigma-Aldrich, Taufkirchen, Germany) by reacting the OCG-diOHs with IEMA under inert conditions in dichloromethane for 6 d at room temperature, catalyzed by dibutyl tin dilaurate. A detailed description can be found in reference [13]. Copolymer networks based on OCG-diIEMAs (glycolide content of 8, 16, and 26 mol%, ratio 1:1:1 wt%) were synthesized as films by radical copolymerization with azodiisobutyronitrile (AIBN, Taufkirchen, Germany) in dichloroethane (30 wt%) at 70 °C for 24 h. The films were obtained by injecting the solution with a syringe between two glass plates covered with hostaphan rm 100 foil and a 1 mm distance holder made from polytetrafluorethylene. The obtained polymer networks were extracted with chloroform and were dried under vacuum until constant weight was achieved.

Degradation experiments

Polymer networks (standard test specimens, ISO 527-2/1BB) were programmed with a tensile tester (Zwick Z1.0, Ulm, Germany) equipped with a thermo-chamber and a temperature controller (Eurotherm Regler, Limburg, Germany). In the programming procedure, samples were elongated at 60 °C to 200% with a strain rate of 5 mm·min⁻¹. The temperature was decreased to 0 °C after 10 min with a cooling rate of 10 K·min⁻¹ under constant strain. Afterwards, the stress was released. Samples in the programmed shape (200% of elongation) were incubated in a phosphate buffer saline solution (pH = 7.4) at 40 °C. Samples were removed from the solution at certain time intervals, were washed with distilled water to remove salts of the buffer solution, were dried, and were characterized by the remaining sample mass (m_{re}), swelling (Q) in chloroform, differential scanning calorimetry (DSC), and cyclic, thermomechanical tensile tests. Margin of errors from degradation experiments were determined by dividing the partially degraded sample into three subsamples.

Characterization methods

¹H-NMR spectra were recorded at 25 °C in CDCl₃ with a Bruker Avance 500 spectrometer (500 MHz, Bruker, Karlsruhe, Germany) with a relaxation time of 2 seconds.

Multidetector gel permeation chromatography was performed on a system (GPC) consisting of a precolumn, two 300 × 0.8 mm M columns (PSS, Mainz, Germany), an isocratic pump 2080, an automatic injector AS 2050 (both Jasco, Tokyo, Japan), a RI detector Shodex RI-101 (Showa Denko, München, Germany), and a dual detector T60A (Viscotek Corporation, Houston, USA) using chloroform (0.2 wt% toluene as internal standard, 35 °C, 1.0 mL·min⁻¹) as eluent. Number average of molecular weight (M_n) of the

copolymers were calculated from the GPC system operated in universal calibration using Mark-Houwink equation. Polystyrene samples were used to determine the hydrodynamic volume as function of elution volume.

For the determination of the remaining sample mass (m_{re}) and the swelling in chloroform (Q), samples were extracted with chloroform for three times and dried until constant weight was achieved. The remaining sample mass was determined by comparing the weight before and after extraction. The degree of swelling in chloroform was calculated as the ratio between the sample mass swollen in chloroform and after extraction in the dry state.

DSC experiments for non-degraded and degraded samples were performed on a Netzsch DSC 204 Phoenix (Netzsch, Selb, Germany) in the temperature range between -100 °C and 100 °C with heating and cooling rates of 10 K·min⁻¹ and a waiting period of 2 min between heating and cooling runs in sealed aluminium pans. Both heating runs were analyzed. Degraded samples were dried before analysis. The margin of error resulted from subdividing on sample into 3 pieces and measuring each.

Cyclic, thermomechanical tensile tests were performed on standard test specimens (ISO 527-2/1BB), which were prepared by punching from a film, with a tensile tester (Zwick Z1.0, Ulm, Germany) equipped with a thermo-chamber and a temperature controller (Eurotherm Regler, Limburg, Germany). After degradation experiments, tensile tests were performed on dried samples by subsequent actuation cycles between 40 °C as T_{sep} and 0 °C as T_{low} on standard test specimens (ISO 527-2/1BB) of copolymer networks in the stress free state without an additional programming of samples. Reversible elongation (ϵ_{rev}) was determined by equation 1, where l_B and l_A are the lengths of the copolymer network at T_{low} and T_{sep} , respectively. Values are mean average values of 3 samples.

$$\epsilon_{rev} = \frac{l_B - l_A}{l_B} \cdot 100 \quad (1)$$

RESULTS AND DISCUSSION

Synthesis of Polymer Networks Based on Oligo[ϵ -caprolactone)-co-glycolide]

The co-oligoesters OCG(x) were synthesized by ring-opening polymerization of ϵ -caprolactone and diglycolide (x represents the glycolide content) utilizing butandiol as initiator and dibutyltin oxide as catalysts as presented in Figure 1. The glycolide content of the oligomers was varied between 10 and 30 mol% in order to enable the design of copolymers with significantly different thermal transitions as well as a fast degradation behaviour. As the integration of glycolide would strongly affect the thermal properties [14], the molecular weight was kept constant for the copolymers (calculated to be 10.0 kg·mol⁻¹).

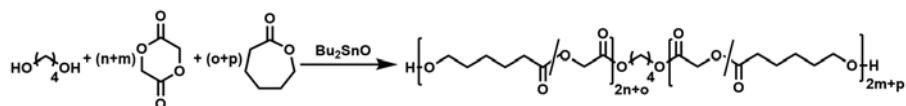


Figure 1. Synthesis scheme of the ring-opening polymerization of ϵ -caprolactone and diglycolide utilizing butanediol as initiator and dibutyltin oxide as catalyst and assignment of signals.

The composition of the synthesized copolymers was investigated by $^1\text{H-NMR}$ spectroscopy from which a glycolide content of 8 ± 2 mol% for OCG(8), 16 ± 2 mol% for OCG(16), and 26 ± 2 mol% for OEG(26) could be determined (Table 1). The sequence structure of copolymers could also be analysed by NMR spectroscopy, by determining the ratios of the specific triads and dyads in the different copolyesters. The peak at a chemical shift of 4.75 ppm could be attributed to the CH_2 -group of glycolide (G) in a neighbourhood of G-G-G. When a G unit is directly linked to ϵ -caprolactone (C), the peak is shifted to a higher field (4.64 ppm for G-G-C and 4.53 ppm for C-G-C). A representative spectrum for assignment is shown in Fig. 2. Triads were calculated according to equation 1:

$$\text{ratio of triad } x = I(\text{triad } x) \cdot [I(\text{triad}_{\text{CGC}}) + I(\text{triad}_{\text{CCG}}) + I(\text{triad}_{\text{GGG}})]^{-1} \cdot 100 \quad (1)$$

in which I represents the integral.

As result of the raised glycolide content within the co-oligoesters the character of a random structure increased with increasing glycolide amount. The distribution of dyads was analysed by comparing the peak integrals from the CH_2 -group of the C unit ($\text{CH}_2\text{-COO}$) at 2.24 ppm (C-C) and at 2.37 ppm (G-C). Dyads were calculated according to equation 2:

$$\text{ratio of dyad } x = I(\text{dyad } x) \cdot [I(\text{dyad}_{\text{CG}}) + I(\text{dyad}_{\text{CC}})]^{-1} \cdot 100 \quad (2)$$

in which I represents the integral.

Hence, also the investigation of the dyad ratio suggested an increasing character of a random copolymer structure with an increasing content of glycolide.

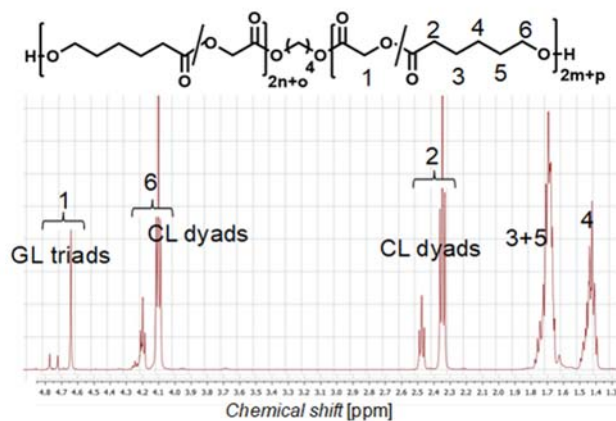


Figure 2: Chemical shifts and assignments of dyads and triads. $^1\text{H-NMR}$ (500 MHz, CDCl_3): δ [ppm] = 4.57-4.85 (m, CH_2 -1); 3.65-4.26 (m, CH_2 -initiator and -6); 2.28-2.47 (m, CH_2 -2); 1.61-1.75 (m, CH_2 -3, and -5); 1.25–1.48 (m, CH_2 -initiator and -4).

Table 1. Determination of glycolide content, triad and dyad ratio, analysis of molecular weight (M_n) and dispersity (D), and investigation of melting temperatures (T_m s) of synthesized OCG copolymers.

Sample- ID	glycolide content ^[a]	triad ratio ^[a]	dyad ratio ^[a]
	[mol%]	C-G-C : C-G-G : G-G-G	C-C : G-C
OCG(8)	8 ± 2	$92 \pm 5 : 7 \pm 1 : 1$ (132 : 12 : 1)	$91 \pm 5 : 9 \pm 1$ (85 : 15)
OCG(16)	16 ± 2	$82 \pm 5 : 17 \pm 2 : 1$ (27 : 5 : 1)	$79 \pm 4 : 21 \pm 2$ (71 : 27)
OCG(26)	26 ± 2	$78 \pm 4 : 21 \pm 2 : 1$ (1:1:1)	$71 \pm 4 : 29 \pm 2$ (55 : 38)
Sample- ID	M_n ^[b]	D	T_m ^[c]
	[kg·mol ⁻¹]		[°C]
OCG(8)	11.0 ± 1.1	1.6	49 ± 2
OCG(16)	10.0 ± 1.0	1.6	39 ± 2
OCG(26)	10.5 ± 1.1	1.6	27 ± 2

a) Determined by ^1H NMR spectroscopy in chloroform according to the equation: glycolide content = $I(\text{CH}_2\text{-G}) \cdot [I(\text{CH}_2\text{-G}) + I(\text{CH}_2\text{-C})]^{-1} \cdot 100$, margin of error results from error of method estimated to be 3% of integral

b) Determined by universally calibrated GPC using chloroform as eluent, $n = 3$

c) Determined from DSC measurements between -100 and 100 °C from the 2nd heating run, $n = 3$

The molecular weights (M_n) of the synthesised OCG were investigated by GPC measurements. Here, in agreement with the calculated molecular weight (10.0 kg·mol⁻¹) by adjusting the initiator to monomer ratio, the synthesized co-oligoesters exhibited a M_n between 10.0 and 11.0 kg·mol⁻¹ and a low dispersity about 1.6. The melting temperatures (T_m s) of the different co-oligoesters were analysed by DSC measurements in the second heating run. Here, a distinct influence of the glycolide content on the melting transition was detected and T_m decreased when the glycolide content was increased. This decrease was attributed to the increasing sterical hindrance of oligo(ϵ -caprolactone) crystallization when glycolide units are incorporated into the polymer chains, which will be more pronounced as higher the random sequence character of the copolymer is. As the thermal transition of OCGs was highly dependent on the glycolide content, copolymers including a high amount of fast degrading glycolide units (like OCG(26)) will preferentially act as actuator domain (domain with a lower T_m in comparison to the skeleton domain), whereby the content of glycolide units within the skeleton domain will be less pronounced (as present within OCG(8)).

In a subsequent synthesis step, the co-oligoesters were converted with 2-isocynoethyl methacrylate (IEMA) in an addition reaction to obtain dimethacrylated OCGs. All IEMA functionalized co-oligoesters provided a degree of end group functionalization above 96% as detected by NMR spectroscopy and in this way were qualified for the synthesis of OCG based actuators (thermal properties were not affected by the end group functionalization).

In order to realize a broad melting transition (which can be divided into actuator and skeleton domain) in the polymeric network, the different IEMA functionalized co-oligoesters OCG(8), OCG(16), and OCG(26) were utilized in a ratio of 1:1:1 for network synthesis. The created networks system exhibited a gel content of $87 \pm 2\%$ and a swelling in chloroform about 1300 ± 100 wt%. According to the combination of OCGs providing

distinct separated melting transitions, the copolymer network provided a melting range with $\Delta T = 17\text{ }^{\circ}\text{C}$ and a T_m of $39 \pm 1\text{ }^{\circ}\text{C}$ (Fig. 3). By means of tensile tests at $60\text{ }^{\circ}\text{C}$, the elongation at break was detected ($\epsilon_b = 290 \pm 20\%$), whereby a deformation about 200% was selected for the programming procedure as required for the actuation capability.

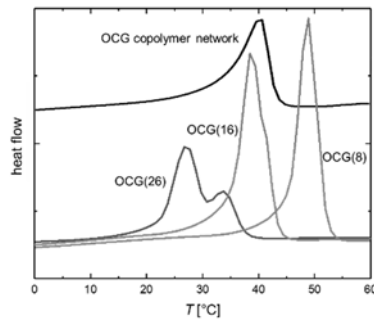


Figure 3. Thermograms of the second heating run of the IMEA functionalized OCG copolyesters as well as the OCG copolymer network.

Hydrolytic Degradation of Oligo[ϵ -caprolactone]-co-glycolide] Actuators

Hydrolytic degradation experiments utilizing PBS buffer ($\text{pH} = 7.4$) were performed on OCG copolymer networks in their programmed state. Therefore, the polymeric networks were elongated by 200% at $60\text{ }^{\circ}\text{C}$ (above the melting transition) and were cooled to $0\text{ }^{\circ}\text{C}$. Afterwards, the stress was released and the temporary shape was obtained. The degradation experiments were carried out at a temperature of $40\text{ }^{\circ}\text{C}$, which is located within the broad melting transition of the copolymer network (offset of thermal transition about $44\text{ }^{\circ}\text{C}$). Hence, a loss of actuator characteristic induced by heating above the whole melting transition is avoided and the shape A of the actuator material is obtained. Fig. 4 displays representative images of samples before and during degradation.



Figure 4. Standard test specimens, after programming and reversible actuation and 11 d after degradation.

The determination of the remaining sample mass (m_{re}) and the swelling capacity (Q) of the OCG network in the swelling media chloroform is presented in Figure 5 as function of degradation time.

A rapid decrease in the sample mass of the created OCG networks as function of time was detected. Simultaneously the swelling behaviour in chloroform drastically increased. The actuator system exhibited an almost linear decrease in the remaining sample mass from 99 ± 1 wt% (start of degradation experiment) to 51 ± 2 wt% after 21 days of hydrolytic degradation (correlates to a mass loss about 49 wt%). In comparison to reported degradable actuators based on oligo(ϵ -caprolactone), where a mass loss of only 25 wt% was detected within 105 days of degradation (under accelerated conditions at pH = 13 in the programmed state), the designed OCG actuators provided a significantly higher rate of degradation (at pH = 7.4), which was related to the fast degradability of the including glycolide units. In addition, Q of OCG networks in chloroform as swelling medium increased from 1300 ± 100 wt% (start of degradation) to 2600 ± 200 wt% (21 days of degradation). This increase in Q indicated the increasing polymer mesh size as result of a decrease in netpoint density.

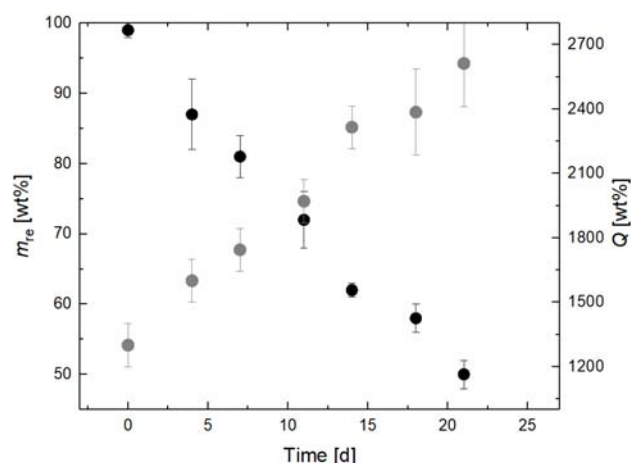


Figure 5. Degradation experiments at 40 °C in PBS buffer with determination of the remaining sample mass (m_{re} , ●) and degree of swelling (Q , ●) in chloroform. Error bars represent the standard deviation of three samples.

Influence of Degradation on Thermal Properties

The hydrolytic degradation of the created OCG copolymer networks resulted in a reduced sample mass and increase in polymer mesh size. In order to investigate how the crystalline domains as required for the actuation capability will be affected by the polymer chain scission and release of cleaved fractions of the polymeric network, the thermal properties were analysed during degradation experiments. In Figure 6, the two melting transitions ($T_{m,1}$ and $T_{m,2}$), which were detected in the first heating run are presented. These thermal transitions were generated during the degradation experiment at 40 °C (according to the thermal history) and represent the crystalline fractions related to the actuation domain ($T < 40$ °C, $T_{m,1}$) and to the skeleton domain (above 40 °C, $T_{m,2}$). Here, $T_{m,1}$ exhibited a slight decrease from 39 ± 1 °C to 37 ± 1 °C within 21 days of degradation and simultaneously $T_{m,2}$ increased from 50 ± 1 °C to 53 ± 1 °C. As the kinetics of hydrolytic degradation of ester groups is faster in amorphous regions and the degradation experiment

is performed with actuators in their shape A (at 40 °C, actuation unit is amorphous), the hydrolytic cleavage preferentially occurs within copolymers generating the actuator domains. As result of degradation and decrease in polymer chain length, the crystallization process is hindered, whereby $T_{m,1}$ is decreased. In addition, copolymers of ϵ -caprolactone and glycolide with a random sequence structure are not able to provide crystalline domains of glycolide when the content is below 60 mol% [15]. Hence, the cleavage of ester groups will preferentially occur within glycolide units and the degradation will be more pronounced for OCGs with a higher glycolide content (providing a lower T_m). As result, an increase in $T_{m,2}$ of the skeleton forming domain (semi-crystalline at the temperature of degradation) is obtained.

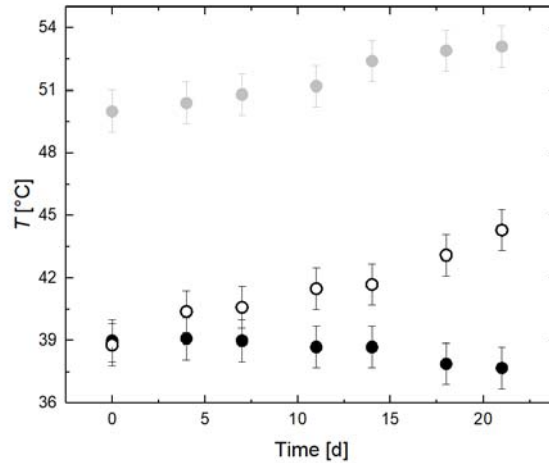


Figure 6. Thermal properties of OCG networks as function of hydrolytic degradation with $T_{m,1}$ (●) and $T_{m,2}$ (●) of the first DSC heating run, as well as T_m (○) of the second DSC heating run. Given errors indicate the error of DSC measurements related to the experimental setup.

A cleavage of copolymer chains providing a lower crystal size with the resulting increase in the overall crystal size was also detected in the second heating run of DSC measurements (thermal history of degradation experiment is not affecting T_m). As presented in Figure 6, the thermal transition increased from 39 ± 1 °C (undegraded material) to 44 ± 1 °C after 21 days of degradation. This increase in T_m significantly demonstrates the change of the crystal size ratio towards crystalline domains with higher crystal dimensions. Furthermore, it has to be mentioned that the degradation within the copolymer chains would increase the chain mobility within the polymeric network, whereby the generation of additional crystalline fractions might be enabled.

Influence of Degradation on Actuation Capability

The hydrolytic degradation of OCG networks resulted in changed thermal properties, whereby also a significant influence of the degradation on the actuation capability is expected. The actuation of the copolymer network was analysed in a temperature interval between 40 °C as T_{sep} and 0 °C as T_{low} under stress free conditions.

The heating and cooling cycles of the designed OCG actuator at a degradation time of 0, 4, 7, and 11 days are presented in Figure 7. Here, the illustrated reversible movement as result of crystallization induced elongation at 0 °C (deformation of $10.4 \pm 0.7\%$ in relation to the sample dimension at the beginning of measurement) and melting induced contraction at 40 °C (deformation of $-2.5 \pm 1.1\%$) correlated to a reversible elongation (ϵ_{rev}) of $10.2 \pm 0.5\%$ (calculated according to equation 1). When the OCG polymer networks were hydrolytically degraded at pH = 7.4 for 4 days, the reversible movement was significantly reduced ranging from $6.2 \pm 0.6\%$ (at 0 °C) to $-1.1 \pm 0.4\%$ (at 40 °C) with $\epsilon_{rev} = 5.7 \pm 0.4\%$. After 7 days of degradation, the reversible movement furthermore decreased between $3.2 \pm 0.5\%$ (at 0 °C) and $-0.1 \pm 0.3\%$ (at 40 °C) with $\epsilon_{rev} = 3.1 \pm 0.3\%$. At a degradation time of 11 days, only a heating induced elongation (thermal expansion with a deformation of $0.9 \pm 0.4\%$ at 40 °C) and a cooling induced contraction (thermal shrinking with a deformation of $-0.3 \pm 0.2\%$ at 0 °C) was obtained, which are not related to the actuation capability. Therefore, the loss of actuation capability within 11 days of hydrolytic degradation was detected by means of cyclic, thermomechanical tensile tests. Here, a mass loss about 26 ± 3 wt% was obtained, which was comparable to the change in sample mass (25 wt%) required to lose functionality as detected for actuator materials based on oligo(ϵ -caprolactone).

The hydrolytic degradation of ester groups occurs preferentially within amorphous regions and the degradation experiment is performed at 40 °C, at which the actuation domain is amorphous. The cleavage of glycolide ester groups within the actuating unit results into the reduction of OCGs chains connected via two crosslinks to the polymeric network and the generation of dangling OCG chains (side chains). In this case, a decreasing polymer chain orientation within the actuation domain is obtained, whereby the crystallization process becomes independent from the geometric information of the skeleton domain. Hence, the capacity of crystallization induced elongation and melting induced contraction is reduced resulting in the loss of functionality as detected within 11 days.

Furthermore, as result of the temperature intended for the degradation experiment, the fixation of the actuator system was reduced from $196 \pm 3\%$ to $54 \pm 4\%$. Here, the crystalline domains acting as temporary netpoints within the actuation domain were released resulting in a partial recovery to the permanent shape. The fixation of the OCG polymer networks also decreased as function of time from $54 \pm 4\%$ (start of degradation experiment) to $21 \pm 4\%$ (11 days of degradation), which was related to the cleavage of OCG chains within the skeleton domain. Hence, the hydrolytic degradation of glycolide units is also present within the skeleton domain, which is semi-crystalline at 40 °C. Here, the cleavage of OCG chains results also in the formation of side chains, whereby the degree of chain orientation and consequently the amount of geometric information stored within the actuator material is reduced. As the fixation of the material decreases as function of time, but is still present at 11 days of degradation, it becomes apparent that the degradation within the skeleton domain decreases the performance of reversible actuation, but the loss of actuation is the result of the hydrolytic degradation within the actuation domain.

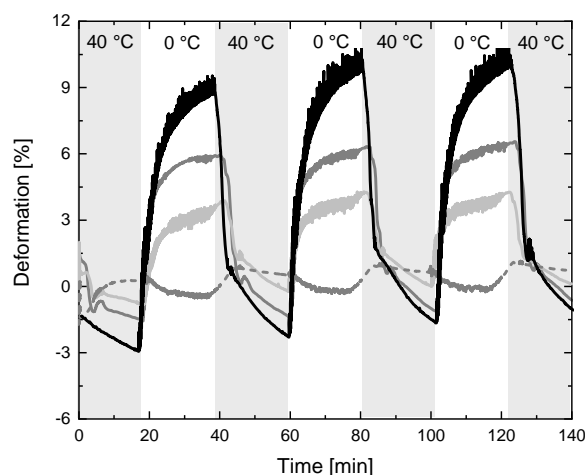


Figure 7. Cyclic, thermomechanical tensile tests of OCG polymer networks as function of degradation time. 0 days (—), 4 days (—), 7 days (—), and 11 days (- -).

CONCLUSION

Shape-memory polymer actuators based on random copolymers from ϵ -caprolactone and diglycolide are multifunctional materials providing reversible macroscopic shape shifts as well as hydrolytic degradability. These materials were hydrolytically degraded utilizing a PBS buffer (pH = 7.4) at $T_{sep} = 40\text{ °C}$ in order to analyse the function-function interdependencies, which will determine the performance of the actuation capability and the material life time. The material mass decreased as result of degradation to 51 wt% within 21 days. Within this time period also the thermal transition of the semi-crystalline copolymer networks were affected resulting in a decrease of T_m of the actuator domain and an increase of T_m of the skeleton domain. The change in sample mass and thermal properties furthermore influenced the actuation performance of the material system, whereby the loss of reversible actuation was detected within 11 days of degradation. Here, the cleavage of glycolide units within the skeleton domain decreases the performance of the actuation capability according to a reduction of polymer chain orientation. Simultaneously, the hydrolytic degradation within the actuation domain resulted in the loss of functionality as the directed crystallization was hindered by the formation of dangling chain ends. In this way, the type and content of easily hydrolyzable ester bonds within the actuation domains are capable to control simultaneously the degradation behaviour and the actuation performance.

ACKNOWLEDGMENTS

This work was financially supported by the Helmholtz Association through program-oriented funding and has received funding from the European Union's Horizon 2020 research and innovation programme under grant agreement No. 824074 (GrowBot). The content of this publication is the sole responsibility of the authors. The European

Commission or its services cannot be held responsible for any use that may be made of the information it contains.

References

1. A. Lendlein, M. Balk, N. A. Tarazona and O. E. C. Gould, *Biomacromolecules* **20** (10), 3627-3640 (2019).
2. C. Majidi, *Soft Robotics* **1** (P), 5-11 (2013).
3. A. Miriyev, K. Stack and H. Lipson, *Nature Communications* **8** (1), 596 (2017).
4. L. Hines, K. Petersen, G. Z. Lum and M. Sitti, *Advanced Materials* **29** (13), 1603483 (2017).
5. J. Shintake, V. Cacucciolo, D. Floreano and H. Shea, *Advanced Materials* **30** (29), 1707035 (2018).
6. B. Jin, H. Song, R. Jiang, J. Song, Q. Zhao and T. Xie, *Science Advances* **4** (1), eaao3865 (2018).
7. F. Ge, X. Lu, J. Xiang, X. Tong and Y. Zhao, *Angewandte Chemie International Edition* **56** (22), 6126-6130 (2017).
8. A. Lendlein and O. E. C. Gould, *Nature Reviews Materials* **4** (2), 116-133 (2019).
9. H. Song, Z. Fang, B. Jin, P. Pan, Q. Zhao and T. Xie, *ACS Macro Letters* **8** (6), 682-686 (2019).
10. M. Balk, M. Behl and A. Lendlein, *MRS Advances* **4** (21), 1193-1205 (2019).
11. S. Li, P. Dobrzynski, J. Kasperczyk, M. Bero, C. Braud and M. Vert, *Biomacromolecules* **6** (1), 489-497 (2005).
12. M. Balk, M. Behl, J. Yang, Q. Li, C. Wischke, Y. Feng and A. Lendlein, *Polymers for Advanced Technologies* **28** (10), 1278-1284 (2017).
13. M. Saatchi, M. Behl, U. Nochel and A. Lendlein, *Macromolecular rapid communications* **36** (10), 880-884 (2015).
14. P. Dobrzynski, S. Li, J. Kasperczyk, M. Bero, F. Gasc and M. Vert, *Biomacromolecules* **6** (1), 483-488 (2005).
15. J. W. Pack, S. H. Kim, I.-W. Cho, S. Y. Park and Y. H. Kim, *Journal of Polymer Science Part A: Polymer Chemistry* **40** (4), 544-554 (2002).